

This is the accepted manuscript made available via CHORUS. The article has been published as:

Nature and topology of the low-energy states in ZrTe_5

L. Moreschini, J. C. Johannsen, H. Berger, J. Denlinger, C. Jozwiak, E. Rotenberg, K. S. Kim,
A. Bostwick, and M. Grioni

Phys. Rev. B **94**, 081101 — Published 4 August 2016

DOI: [10.1103/PhysRevB.94.081101](https://doi.org/10.1103/PhysRevB.94.081101)

Nature and topology of the low energy states in ZrTe_5

L. Moreschini,^{1,2,3,*} J. C. Johannsen,^{1,4} H. Berger,⁴ J. Denlinger,¹ C. Jozwiack,¹ E. Rotenberg,¹ K. S. Kim,^{2,3} A. Bostwick,¹ and M. Grioni⁴

¹*Advanced Light Source (ALS), Lawrence Berkeley National Laboratory, Berkeley, California 94720, USA*

²*Département of Physics, Pohang University of Science and Technology, Pohang 790-784, Korea*

³*Center for Artificial Low Dimensional Electronic Systems,*

Institute for Basic Science, Pohang 790-784, Korea

⁴*Institute of Condensed Matter Physics (ICMP),*

Ecole Polytechnique Fédérale de Lausanne (EPFL), CH-1015 Lausanne, Switzerland

Long known for its peculiar resistivity, showing a thus far unexplained anomalous peak as a function of temperature, ZrTe_5 has recently received rising attention in a somewhat different context. While both theoretical and experimental results seem to point to a non trivial topology of the low energy electronic states, there is no agreement on the nature of their topological character. Here, by an angle resolved photoemission study of the evolution of the band structure with temperature and surface doping, we show that i) the material presents a van Hove singularity close to the Fermi level, and ii) no surface states exist at the (010) surface. These findings reconcile band structure measurements with transport results and establish the topology of this puzzling compound.

The first research examples on zirconium pentatelluride ZrTe_5 date from the beginning of the eighties. In those initial studies the source of interest was a peculiar behavior of the electronic transport with temperature. At low temperature the resistivity follows a metallic curve, but it peaks at $T^* \simeq 150\text{K}$ and acquires a semiconducting response. At higher temperatures it assumes a slightly positive dependence, reminiscent of a (very poor) metal¹⁻³. Lacking evidence for structural or electronic reconstructions⁴, such as a charge density wave, there is at present no explanation for these observations. Transport data are complemented by thermoelectric measurements, which attribute negative sign to the charge carriers at $T < T^*$ and positive sign above T^* ^{5,6}. Shubnikov-de Haas experiments at $T \ll T^*$ yield conflicting results. In one case three Fermi level crossings were found, assigned to one hole (largest) and two electron (medium and smallest) pockets⁷. This would guarantee a semimetal with charge compensation, called for by the even number of p electrons in Te. Another group finds a single Fermi surface⁸, and therefore no possible compensation. Theoretical calculations support a semimetallic state at low temperature, with the low energy bands centered at the Γ -Z line of the Brillouin zone (BZ)^{9,10}.

Much more recently, with the rise of topological insulators (TI), an intense activity on ZrTe_5 resumed from a different perspective. Magnetotransport measurements^{11,12} and optics¹³ appear to be consistent with the presence of three-dimensional (3D) Dirac fermions, which would set this material within the novel class of 3D Dirac semimetals^{14,15}. Theory favors instead a gapped electronic structure with band inversion, which translates in single-layer ZrTe_5 being (ideally) a 2D TI and bulk ZrTe_5 being at the phase boundary between a strong and a weak TI. The interlayer spacing is believed to play a key role in defining the topological character of the bulk material^{16,17}.

The few angle resolved photoemission (ARPES) in-

vestigations available to this point^{6,11,18-20} agree on the general band mapping of the material, but diverge very evidently in their descriptions of the low energy states. This letter focuses on the low energy electronic structure and its modifications upon temperature and surface doping, pointing out relevant elements which have been overlooked and providing experimental evidence for the topological classification of ZrTe_5 as either a weak TI or a trivial semiconductor.

The crystal structure, shown in Fig. 1(a), consists of chains of Zr atoms embedded in trigonal Te prisms and running along the a axis. The two remaining Te atoms per formula unit bridge two adjacent chains along the c axis. Such pattern forms layers which are then weakly coupled along b by van der Waals forces. The primitive unit cell size is one layer wide in the b direction, and the corresponding reciprocal space is filled with prisms as sketched in Fig. 1(b), elongated along a^* and stacked along b^* . It is convenient to use a base-centered orthorhombic cell, shown in Fig. 1(a), which contains instead two layers. The only difference between one layer and the neighboring ones is a translation along a by half the Zr-Zr distance.

The crystals break easily along both the ab and ac planes parallel to the chains, but produce surfaces of measurable size only along ac , i.e., at the (010) surface. Throughout this paper, in order to maintain the conventional ARPES definition of k_z as oriented normal to the sample surface, we define x , y and z as directed along a , c and b , respectively. The data were collected on the MAESTRO and MERLIN beamlines at the ALS²¹.

Fig. 1(c-e) shows an overview of the band structure measured along the three high-symmetry directions through Γ in the $k_x k_y$ plane. The top of the valence band (VB) consists of hole-like states yielding the characteristic constant energy contours shown in Fig. 1(g) and already observed in previous work¹¹. A preliminary consideration concerns the dimensionality of the material. Whereas structurally it appears clearly one dimensional

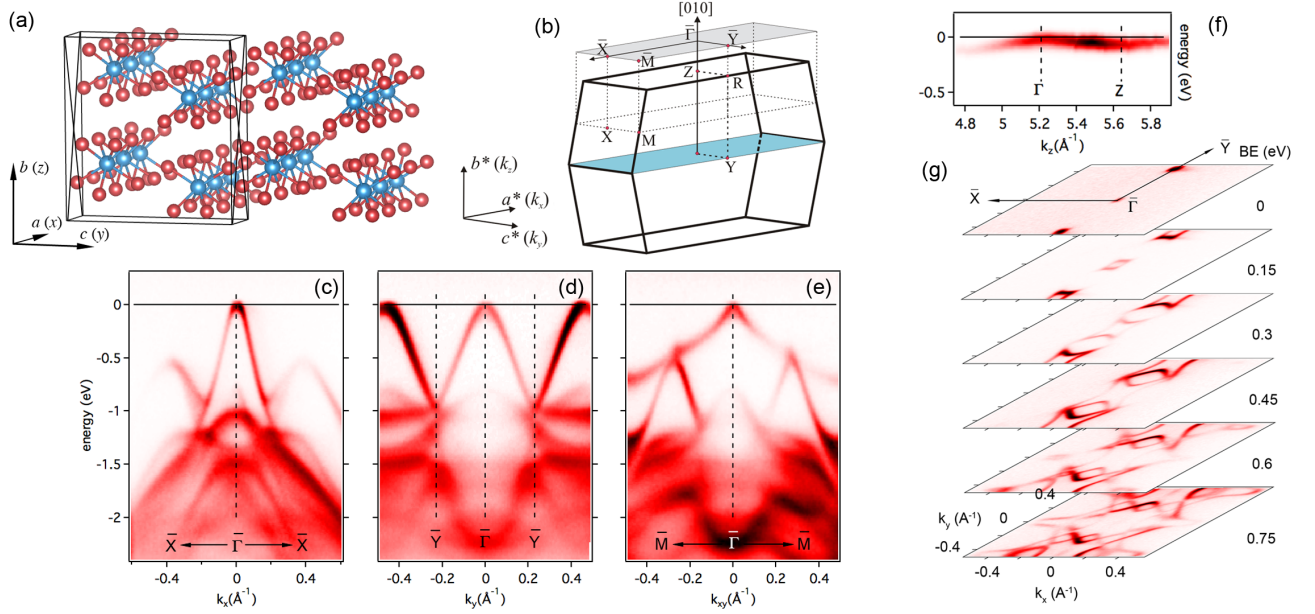


FIG. 1: (a) real space view of ZrTe₅, with Zr and Te atoms in blue and red, respectively, with the conventional unit cell; (b) the 3D BZ with the relevant high-symmetry points. The dark-colored and light-colored planes represent the $k_x k_y$ plane containing $\bar{\Gamma}$ and the (010) surface BZ, respectively; (c-e) band dispersion measured at $h\nu=69$ eV along the indicated high-symmetry directions; (f) k_z dispersion measured along $\bar{\Gamma}$ - \bar{Z} . $\bar{\Gamma}$ and \bar{Z} correspond here to $h\nu=100$ eV and 118 eV, respectively. The k_z momentum is evaluated using an inner potential V_0 of 7.5 eV; (g) a stack of constant energy cuts taken at the binding energies indicated on the right, for the same dataset of (c-e). All the data are measured at $T \simeq 120$ K. The relevant dimensions are $\bar{\Gamma}\bar{X} = 0.79 \text{ \AA}^{-1}$, $\bar{\Gamma}\bar{Y} = 0.23 \text{ \AA}^{-1}$, $\bar{\Gamma}\bar{M} = 0.82 \text{ \AA}^{-1}$ and $\bar{\Gamma}\bar{Z} = 0.43 \text{ \AA}^{-1}$

with needle-like domains, electronically it shows a nearly 2D behavior. The effective mass along y ($\sim -0.09m_e$) is less than twice as large as that along x ($\sim -0.05m_e$), in line with what observed in transport²², and much smaller than that along z ($\sim -4.5m_e$). The structural properties are probably determined mostly by the Zr chains, which are well separated along y , while electronically the dominant contribution at the top of the VB comes from Te atoms, which form a nearly 2D mesh in the xy plane. Electronically ZrTe₅ can thus be treated as a van der Waals layered material.

The bulk sensitivity at the low energies typically used in ARPES is only a few \AA . Given the large interlayer separation along z , $\sim 7.25 \text{ \AA}$, it may be questioned whether there is any hope at all to see a signal from electrons below the top atomic layer. As shown in Fig. 1(f), even though the electron escape depth may be small, the wavefunctions carry information on the periodicity well beyond such escape depth. Photon energy dependent data present indeed a clear oscillation, sign of a moderate (as expected) but measurable k_z dispersion, downwards from $\bar{\Gamma}$ to \bar{Z} (hole-like).

This was revealed in recent studies^{11,19}, and used to assign the observed states to the bulk band structure, but another relevant aspect went unnoticed. Figure 2(a,b) shows two close-ups of the band structure measured along k_x for the $\bar{\Gamma}$ and \bar{Z} points, respectively. In the former the ARPES intensity engenders a Λ -shaped dispersion, whereas in the latter the top of the band is clearly M-

shaped. This point has, as we shall see, profound consequences for the physics of this material.

A closer inspection of Fig. 2(a) reveals a weaker intensity inside the main parabola. This second state is a backfolded replica of the M-shaped band in \bar{Z} . The ZrTe₅ structure is known to be prone to slight distortions²³, and it is entirely possible that these could be enhanced close to the surface. In x-ray diffraction data a $(1/2, 1/2, 0)$ superlattice in the ab plane was observed, which would fold the electronic states into a reduced BZ, only $2\pi/b$ wide in the k_z direction^{3,24}. This is seen more clearly in a higher resolution and higher statistics version of Fig. 1(f), shown in Fig. 2(c). The weaker state intensity is completely suppressed in the right half of the figure, but can be nicely followed between $\bar{\Gamma}$ and half way to \bar{Z} . Note that, given the very slight amount of distortion, attempts to identify two states as a sign of a bilayer splitting do not seem justified, since the lattice primitive cell contains one single layer.

Although clearly the physics of this material is strongly influenced by temperature, the data appeared so far, with one exception²⁰, are available at sparse temperatures and clearly a systematic study is called for. Figure 2(d-g) shows the k_y dispersion of the VB top for $T \gg T^*$ and $T \ll T^*$. At $\bar{\Gamma}$, the VB maximum is below E_F at high T and shifts well above at low T . At \bar{Z} , where the state has higher binding energy, the intensity peak at 40K does not quite cross E_F yet, and remains instead slightly below. Hence, at low T the band in \bar{Z} is occupied, the one in $\bar{\Gamma}$ is

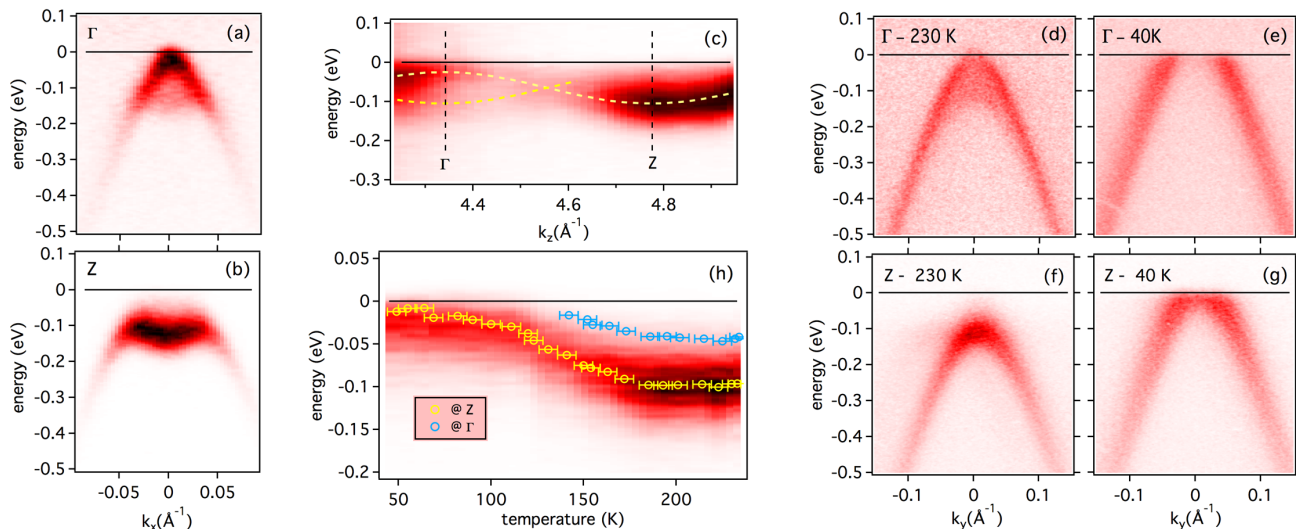


FIG. 2: (a,b) valence band dispersion along k_x , measured at Γ (69 eV) and Z (83.5 eV), at $T \simeq 160$ K; (c) close-up of the k_z dispersion. The dashed curves are sine waves with period $4\pi/b$, shown as guides to the eye. (d-g) valence band dispersion along k_y , measured at Γ (69 eV) and Z (83.5 eV) for high and low T . Note in (d) the clear backfolded replica of the band in (f); (h) a sequence of EDCs measured at Z for decreasing temperature, shown as an image plot. The yellow symbols indicate the peak positions as obtained by a simple Voigt fit. The blue symbols indicate the peak positions of an equivalent dataset measured for Γ , and limited to the range where the fit is reliable. The intensity of the backfolding is weak and does not flaw the analysis. No normalization has been applied to the data

not. This is confirmed by a stack of energy distribution curves (EDCs) measured at Z for decreasing temperatures, shown in Fig. 2(h). The symbols superimposed indicate the fitted peak positions. Another set of symbols indicates, for the subrange of temperatures where the state can be followed, the peak positions obtained by fitting a similar dataset measured at Γ . Limited to this range the curve is an exact translated version of the one at Z and the band shift is therefore rigid. We verified the shift to be reversible.

Most of the change appears to occur monotonically between ~ 100 and ~ 170 K. While a cross comparison between the absolute temperatures may not be wise due to the known influence of defects in the transport properties³, there exist within previous ARPES data clear contradictions, with some authors observing like us a downward shift of the VB between low and high temperature¹⁹, and others claiming exactly the opposite^{6,18,20}. The only other continuous temperature dependence study in a recent preprint shows a monotonous downward shift between room temperature and 2 K²⁰. Those data are also peculiar in that the level of electron doping at low T is even larger than obtained by direct surface doping in Ref. 19. Clearly, extrinsic factors such as the condensation of adsorbates at low temperatures should be carefully considered before attempting a comparison among the existing data, but it seems likely that other elements, such as different defects introduced during the crystal growth, may also play a role in these strong inconsistencies among the different groups.

A key point to notice is that, along k_y , both at Γ and Z the VB is hole-like [Fig. 2(d,f)]. It is instead electron-like

along k_x at Z [Fig. 2(b)]. Therefore, Z is a saddle point for the band dispersion in the $k_x k_y$ plane, and same in the $k_z k_y$ plane since at Z the dispersion is electron-like in k_z as well. In other words, ZrTe_5 presents a 3D van Hove singularity, a possibility hypothesized from optical spectroscopy results¹³, with two electron-like axes. Remember that at low T the only occupied states are those close to Z . The resulting Fermi surface in 3D is too involved to attempt quantitative electron counting simply from the ARPES data, and furthermore, it is possible that the singularity in the density of states will cause some departures from a rigid band shift in the close proximity of E_F which cannot be fully captured by the experiment. However, the presence of a van Hove singularity with two axes of positive effective mass is central, we believe, for establishing a connection between ARPES results and the transport data at low T . Only thanks to the presence of electron-like dispersion along two axes can the Fermi surface consist of electron pockets at low T , in agreement with the negative sign of the carriers observed in thermoelectric measurements^{5,6}.

Note that, while we tried to identify some *consequences* of the observed band shift with temperature, its *origin* remains obscure. Proposals of a strongly asymmetric density of states¹⁹, similarly to the pnictides^{25,26}, seem unlikely given that the states above and below E_F derive here from the same bands, as opposed to pnictides where electrons and holes are found in two entirely different states. Also, the compensation supposed to hold at all temperatures from the even number of p electrons does not seem consistent with our data, since at higher temperatures only the Λ -shaped state presents a Fermi

crossing and no electron pockets can exist. Thus, the description of ZrTe_5 as a p semimetal seems too simplistic and some other source of charge has to play a role.

Studying the temperature dependence of the band structure is unfortunately of little help for determining the topological character of ZrTe_5 . As shown before, the Fermi level moves from slightly above the VB to well within it, so that the conduction band (CB) remains well out of reach. The goal is to discriminate between three proposals appeared thus far: (i) a Dirac semimetal, (ii) a strong TI, and (iii) a weak TI. (i) would result in a bulk Dirac cone centered at Γ , with no bulk gap. (ii) is the most common TI case, with a gapped bulk structure and surface states in every crystallographic direction. (iii) would still have surface states, but only on side surfaces, e.g., at step edges, while in the (010) direction it would look just like a standard semiconductor¹⁶.

We could access the CB states by surface doping with alkali atoms, namely Rb, similar to a recent work where this was achieved by bulk doping using Ta atoms as substitutional defects¹⁹. In general, if the screening length is not too short, the charge transfer from the alkali is effective in shifting down the bands until the density of the unoccupied states is too large to allow further doping. Fig. 3(a) shows the k_x dispersion at Γ after Rb deposition. The EDC in the figure clearly shows a visible tail of the CB at E_F , separated by a dip from the VB²⁷. This is hard to reconcile with (i) above, since a Dirac semimetal should show no gap.

As a further evidence against (i), the energy shift of the Te core levels, shown in Fig. 3(d), after a gradual increase suddenly saturates, as typically observed for semiconductors and insulators^{28,29}. The starting point and

the amount of the shift are irrelevant and depend on the sample temperature, but the saturation point is always the same, and corresponds roughly to the onset of the CB attaining E_F . Assuming a completely symmetric density of states we would deduce a gap of ~ 140 meV if extracted as the peak-to-peak energy separation, but the ARPES estimation of the gap in these conditions should be considered a very coarse one.

Even though no Dirac-like dispersion can be seen within the gap, a definite statement is not possible from Fig. 3(a) as the surface state could have a very different intensity from the bulk bands and be nearly completely hidden. Hence we measured [Fig. 3(b)] the k_x dispersion at Z, where the (backfolded) Λ -shaped state is extremely weak instead. The EDC extracted at Z is completely flat at E_F , with no trace of an additional state. A stack of EDCs over the full Γ -Z range (and beyond) is shown in Fig. 3(c). The statistics is worse than in (a,b) due to time constraints in measuring the whole range without a sizable desorption of Rb from the surface, but small features at the Fermi level (see arrows) can only be found at the photon energies close to Γ . Elsewhere, the EDCs are featureless close to E_F . The presence of a surface state can thus be excluded, and scenario (ii) ruled out.

Our results certainly favor a weak TI as a correct description of ZrTe_5 , or a standard semiconductor in lack of band inversion. However, since ZrTe_5 is supposed to be at the edge between (ii) and (iii)^{16,17}, we cannot dismiss the possibility that the Rb deposition could modify the interlayer separation enough to shift the material from one side to the other of the phase space. The direct measurement of edge states, predicted for a weak TI and rather convincingly shown by tunneling spectroscopy in recent preprints^{19,30}, will be a stimulating challenge for the existing and upcoming nanoARPES facilities.

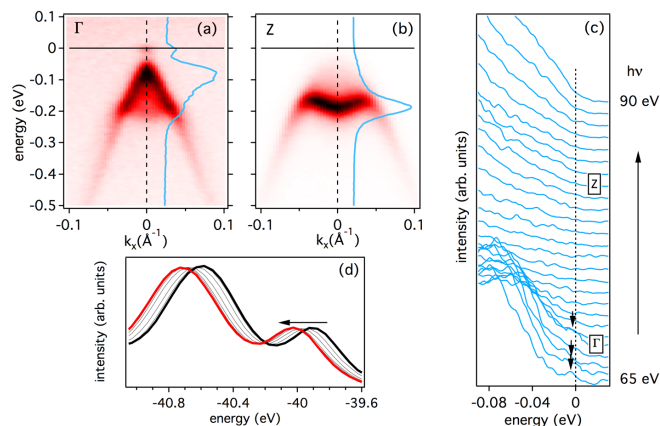


FIG. 3: (a,b) equivalents of Fig. 2(a,b) after deposition of Rb on the sample surface. The spectra superposed to the images are EDCs taken at $k_x = 0$; (c) close-up of a series of (non normalized) EDCs measured for photon energies of 65 eV to 90 eV in steps of 1 eV. The arrows indicate the small intensity at the Fermi level coming from the CB in the vicinity of Γ ; (d) evolution of the Te $5d_{5/2}$ core level at successive steps of the Rb deposition. The thick black and red spectra represent the start and end point of the deposition, respectively.

Acknowledgments

We gratefully acknowledge A. Crepaldi and G. Autès for discussing with us their data during the preparation of this manuscript, M. Gherardi for interesting discussions and Yeongkwan Kim for technical support on MERLIN. The Advanced Light Source is supported by the Director, Office of Science, Office of Basic Energy Sciences, of the U.S. Department of Energy under Contract No. DE-AC02-05CH11231.

-
- * Electronic address: lmoreschini@lbl.gov
- ¹ S. Okada, T. Sambongi, and M. Ido, *Journal of the Physical Society of Japan* **49**, 839 (1980).
 - ² E. Skelton, T. Wieting, S. Wolf, W. Fuller, D. Gubser, T. Francavilla, and F. Levy, *Solid State Communications* **42**, 1 (1982).
 - ³ F. J. DiSalvo, R. M. Fleming, and J. V. Waszczak, *Phys. Rev. B* **24**, 2935 (1981).
 - ⁴ S. Okada, T. Sambongi, M. Ido, Y. Tazuke, R. Aoki, and O. Fujita, *Journal of the Physical Society of Japan* **51**, 460 (1982).
 - ⁵ T. Jones, W. Fuller, T. Wieting, and F. Levy, *Solid State Communications* **42**, 793 (1982).
 - ⁶ D. N. McIlroy, S. Moore, D. Zhang, J. Wharton, B. Kempton, R. Littleton, M. Wilson, T. M. Tritt, and C. G. Olson, *Journal of Physics: Condensed Matter* **16**, L359 (2004).
 - ⁷ G. N. Kamm, D. J. Gillespie, A. C. Ehrlich, T. J. Wieting, and F. Levy, *Phys. Rev. B* **31**, 7617 (1985).
 - ⁸ M. Izumi, T. Nakayama, K. Uchinokura, S. Harada, R. Yoshizaki, and E. Matsuura, *Journal of Physics C: Solid State Physics* **20**, 3691 (1987).
 - ⁹ M. H. Whangbo, F. J. DiSalvo, and R. M. Fleming, *Phys. Rev. B* **26**, 687 (1982).
 - ¹⁰ D. Bullett, *Solid State Communications* **42**, 691 (1982).
 - ¹¹ Q. Li, D. E. Kharzeev, C. Zhang, Y. Huang, I. Pletikosić, A. V. Fedorov, R. D. Zhong, G. A. Schneeloch, G. D. Gu, and T. Valla, *Nat. Phys.* **12**, 550 (2016).
 - ¹² R. Y. Chen, Z. G. Chen, X.-Y. Song, J. A. Schneeloch, G. D. Gu, F. Wang, and N. L. Wang, *Phys. Rev. Lett.* **115**, 176404 (2015).
 - ¹³ R. Y. Chen, S. J. Zhang, J. A. Schneeloch, C. Zhang, Q. Li, G. D. Gu, and N. L. Wang, *Phys. Rev. B* **92**, 075107 (2015).
 - ¹⁴ Z. K. Liu, B. Zhou, Y. Zhang, Z. J. Wang, H. M. Weng, D. Prabhakaran, S.-K. Mo, Z. X. Shen, Z. Fang, X. Dai, et al., *Science* **343**, 864 (2014).
 - ¹⁵ M. Neupane, S.-Y. Xu, R. Sankar, N. Alidoust, G. Bian, C. Liu, I. Belopolski, T.-R. Chang, H.-T. Jeng, H. Lin, et al., *Nature Communications* **5** (2014).
 - ¹⁶ H. Weng, X. Dai, and Z. Fang, *Phys. Rev. X* **4**, 011002 (2014).
 - ¹⁷ O. Yazyev and G. Autès, private communication.
 - ¹⁸ G. Manzoni, A. Sterzi, A. Crepaldi, M. Diego, F. Cilento, M. Zacchigna, P. Bugnon, H. Berger, A. Magrez, M. Gri-
oni, et al., *Phys. Rev. Lett.* **115**, 207402 (2015).
 - ¹⁹ R. Wu, J.-Z. Ma, S.-M. Nie, L.-X. Zhao, X. Huang, J.-X. Yin, B.-B. Fu, P. Richard, G.-F. Chen, Z. Fang, et al., *Phys. Rev. X* **6**, 021017 (2016).
 - ²⁰ Y. Zhang, C. Wang, L. Yu, G. Liu, A. Liang, J. Huang, S. Nie, Y. Zhang, B. Shen, J. Liu, et al. (2016), [arXiv:1602.03576](https://arxiv.org/abs/1602.03576).
 - ²¹ Supplementary information with the scattering geometry is attached to this paper.
 - ²² The anisotropy in the resistivity was reported to grow from ~ 2 up to a ~ 10 at low temperatures (Ref. 4). We tend to believe though that these factors also include extrinsic terms due to the structural mismatch between the different domains along y , which affect the flow of the charge carriers.
 - ²³ D. J. Eaglesham, J. Mulcahy, and J. A. Wilson, *J. Phys. C: Solid State Phys.* **20**, 351 (1987).
 - ²⁴ J. A. Wilson, *Phil. Trans. R. Soc. Lond.* **314**, 159 (1985).
 - ²⁵ R. S. Dhaka, S. E. Hahn, E. Razzoli, R. Jiang, M. Shi, B. N. Harmon, A. Thaler, S. L. Bud'ko, P. C. Canfield, and A. Kaminski, *Phys. Rev. Lett.* **110**, 067002 (2013).
 - ²⁶ V. Brouet, P.-H. Lin, Y. Texier, J. Bobroff, A. Taleb-Ibrahimi, P. Le Fèvre, F. Bertran, M. Casula, P. Werner, S. Biermann, et al., *Phys. Rev. Lett.* **110**, 167002 (2013).
 - ²⁷ The sample was aligned within 0.05 degrees because, with the CB minimum so close to the Fermi level, an apparent gap could be easily produced even by a very slight misalignment.
 - ²⁸ L. Moreschini, G. Autès, A. Crepaldi, S. Moser, J. Johansson, K. Kim, H. Berger, P. Bugnon, A. Magrez, J. Denlinger, et al., *Journal of Electron Spectroscopy and Related Phenomena* **201**, 115 (2015).
 - ²⁹ R. Comin, G. Levy, B. Ludbrook, Z.-H. Zhu, C. N. Veenstra, J. A. Rosen, Y. Singh, P. Gegenwart, D. Stricker, J. N. Hancock, et al., *Phys. Rev. Lett.* **109**, 266406 (2012).
 - ³⁰ X.-B. Li, W.-K. Huang, Y.-Y. Lv, K.-W. Zhang, C.-L. Yang, B.-B. Zhang, Y. B. Chen, S.-H. Yao, J. Zhou, M.-H. Lu, et al., *Phys. Rev. Lett.* **116**, 176803 (2016).